Supporting Information for:

Assessment of Approximate Coupled-Cluster and Algebraic-Diagrammatic-Construction Methods for Ground- and Excited-State Reaction Paths and the Conical-Intersection Seam of a Retinal-Chromophore Model

Deniz Tuna,[1*] Daniel Lefrancois,[2] Łukasz Wolański,[3] Samer Gozem,[4] Igor Schapiro,[5] Tadeusz Andruniów,[3*] Andreas Dreuw,[2*] and Massimo Olivucci[6,7*]

[1] *Max-Planck-Institut für Kohlenforschung, 45470 Mülheim an der Ruhr, Germany*

[2] *Interdisciplinary Center for Scientific Computing, University of Heidelberg, 69120 Heidelberg, Germany*

[3] *Department of Chemistry, Wrocław University of Technology, 50370 Wrocław, Poland*

[4] *Department of Chemistry, University of Southern California, Los Angeles, California 90089, United States*

[5] *Institut de Physique et Chimie des Matériaux de Strasbourg & Labex NIE, Université de Strasbourg, CNRS UMR 7504, Strasbourg 67034, France*

[6] *Department of Chemistry, Bowling Green State University, Bowling Green, Ohio 43402, United States*

[7] *Dipartimento di Biotecnologie, Chimica e Farmacia, Universitá de Siena, 53100 Siena, Italy*

[*] *email: tuna@kofo.mpg.de, tadeusz.andruniow@pwr.wroc.pl, andreas.dreuw@iwr.uni-heidelberg.de, molivuc@bgsu.edu*

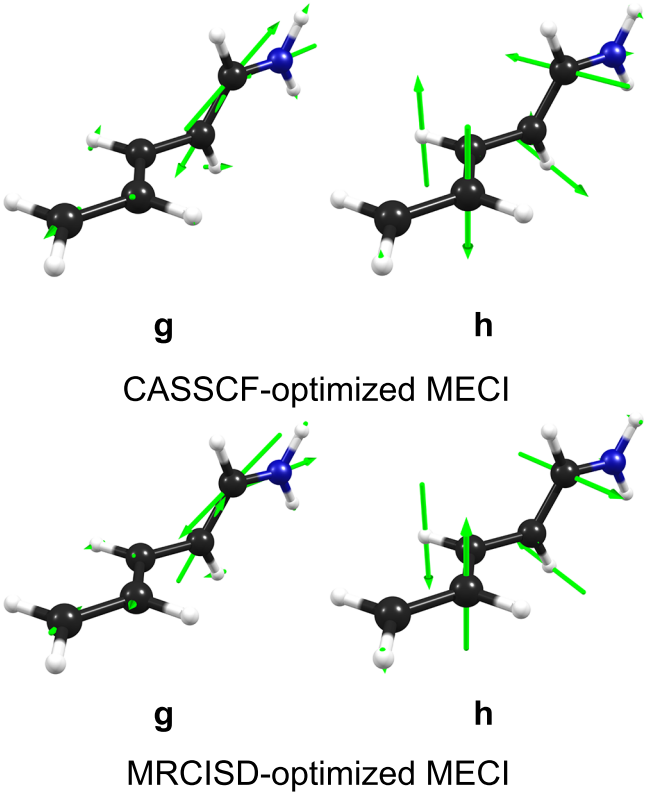

Figure S1 Molecular structures of the CASSCF- and the MRCISD-optimized minimum-energy conical intersection and nuclear-displacement vectors of the orthonormalized branching-space vectors obtained at the CASSCF and MRCISD levels of theory.

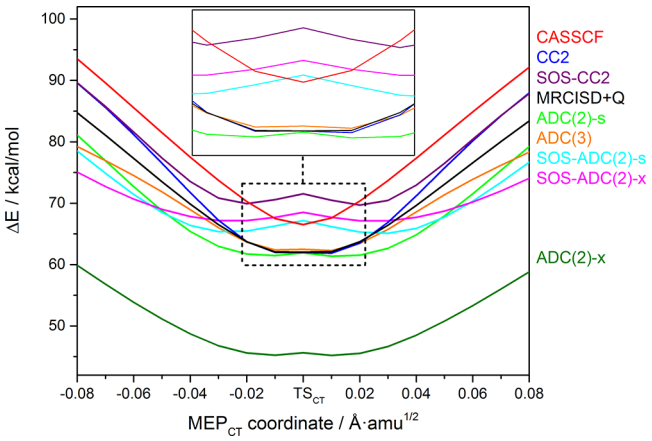

Figure S2 S_1 energy profiles (in kcal/mol relative to *trans*-PSB3) along the MEP_{CT} pathway, which connects TS_{CT} (in the middle of the plot) with *cis*- and *trans*-PSB3. The S_1 energies are given for the CC2 method (blue), the SOS-CC2 method (purple), the ADC(2)-s method (green), the SOS-ADC(2)-s method (cyan), the ADC(2)-x method (olive), the SOS-ADC(2)-x method (magenta), the ADC(3) method (orange), and the reference methods CASSCF (red) and MRCISD+Q (black).

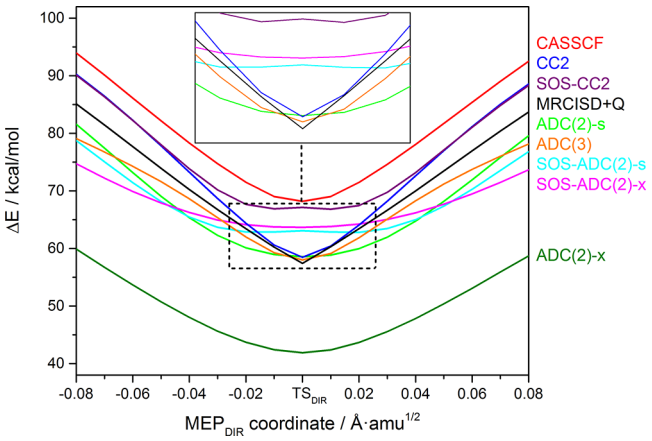

Figure S3 S_1 energy profiles (in kcal/mol relative to *trans*-PSB3) along the MEP_{DIR} pathway, which connects TS_{DIR} (in the middle of the plot) with *cis*- and *trans*-PSB3. The S_1 energies are given for the CC2 method (blue), the SOS-CC2 method (purple), the ADC(2)-s method (green), the SOS-ADC(2)-s method (cyan), the ADC(2)-x method (olive), the SOS-ADC(2)-x method (magenta), the ADC(3) method (orange), and the reference methods CASSCF (red) and MRCISD+Q (black).

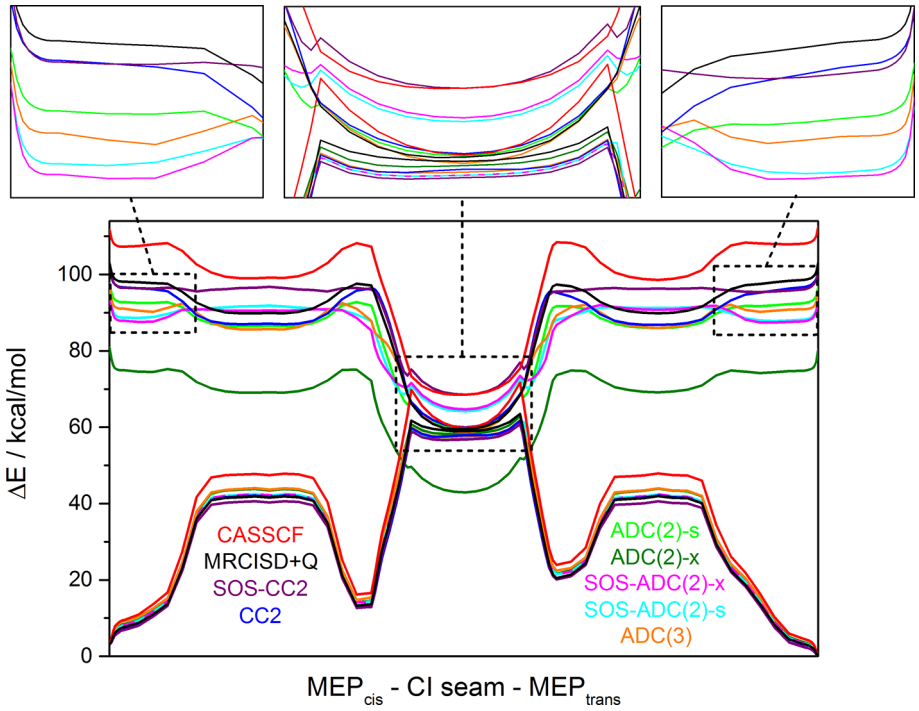

Figure S4 Energy profiles (in kcal/mol relative to *trans*-PSB3) along the composite CASPT2 excited-state pathway, which is composed of the MEP$_{cis}$, the CI seam, and the MEP$_{trans}$ pathways. The S_0 and S_1 energies are given for the CC2 method (blue), the SOS-CC2 method (purple), the ADC(2)-s method (green), the SOS-ADC(2)-s method (cyan), the ADC(2)-x method (olive), the SOS-ADC(2)-x method (magenta), the ADC(3) method (orange), and the reference methods CASSCF (red) and MRCISD+Q (black). The S_0 energies obtained for the ADC(2)-s and ADC(2)-x, as well as for the SOS-ADC(2)-s and SOS-ADC(2)-x methods, respectively, are equal (i.e., they correspond to the MP2 and SOS-MP2 level, respectively), and are given as dashed lines.

Table S1 S_0−S_1 Energy Gaps ($\Delta E_{S_0-S_1}$) at *cis*-PSB3, *trans*-PSB3, CI_{cis}, CI_{BLA}, and CI_{trans} along the Full S1 CASSCF Path (shown in Figure 8 in the article).

method	$\Delta E_{S_0-S_1}$ at *cis*-PSB3	$\Delta E_{S_0-S_1}$ at *trans*-PSB3	$\Delta E_{S_0-S_1}$ at CI_{cis}	$\Delta E_{S_0-S_1}$ at CI_{BLA}	$\Delta E_{S_0-S_1}$ at CI_{trans}
MRCISD+Q	101.4	104.4	6.2	6.6	6.8
MRCISD	104.8	108.1	4.6	4.9	5.0
CASSCF	110.3	114.1	0.0	0.0	0.0
CC2	99.2	101.9	7.9	8.2	8.9
SOS-CC2	100.8	102.7	18.1	18.6	18.9
ADC(2)-s / MP2	95.8	98.2	7.3	7.8	8.3
SOS-ADC(2)-s / SOS-MP2	93.5	95.3	13.5	14.2	14.3
ADC(2)-x / MP2	79.4	82.0	−9.3	−8.6	−8.7
SOS-ADC(2)-x /SOS-MP2	93.8	95.9	14.3	15.3	14.8
ADC(3) / MP3	95.2	97.2	8.1	9.0	8.6

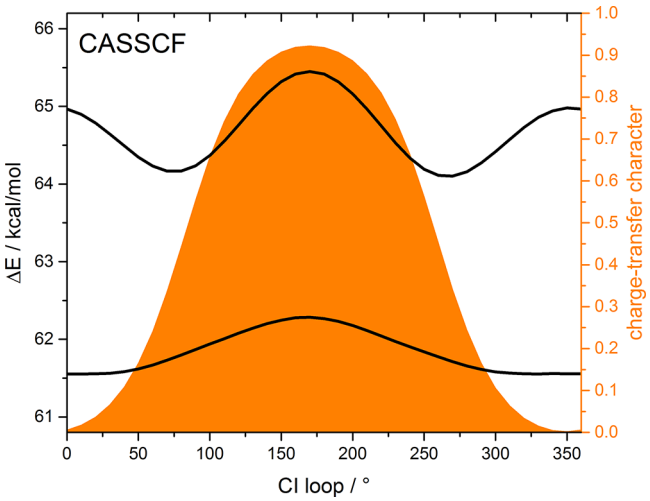

Figure S5 S_0 and S_1 energy profiles (in kcal/mol relative to *trans*-PSB3) for the CASSCF method along the circular path around the S_1/S_0 surface crossing of PSB3. The charge-transfer character of the electronic ground state is shown in orange.

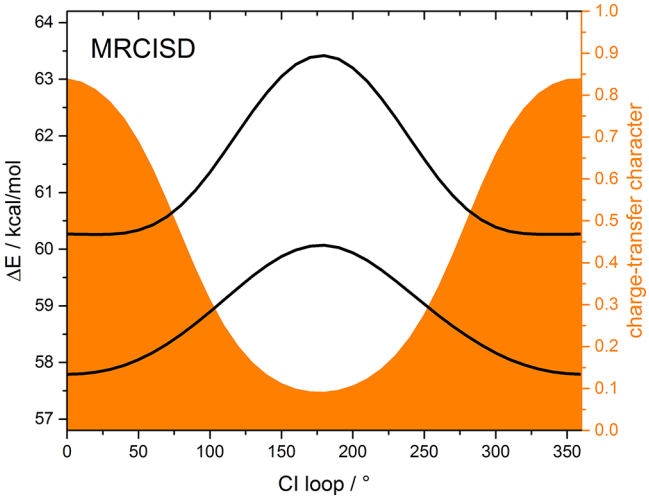

Figure S6 S_0 and S_1 energy profiles (in kcal/mol relative to *trans*-PSB3) for the MRCISD method along the circular path around the S_1/S_0 surface crossing of PSB3. The charge-transfer character of the electronic ground state is shown in orange.

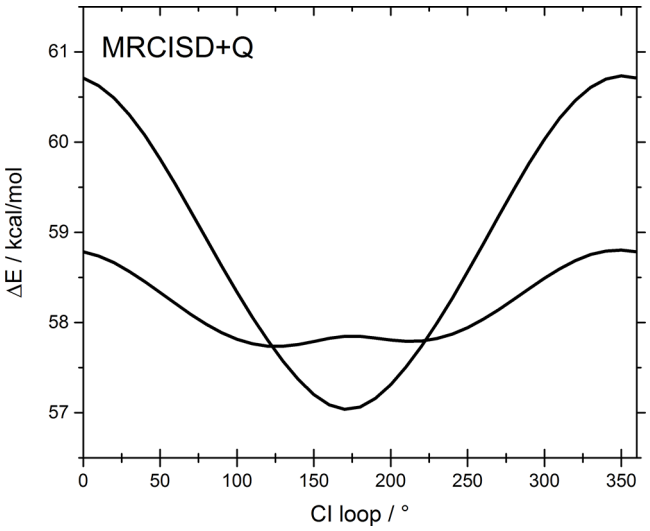

Figure S7 S_0 and S_1 energy profiles (in kcal/mol relative to *trans*-PSB3) for the MRCISD+Q method along the circular path around the S_1/S_0 surface crossing of PSB3. For this circle, we used a radius of 0.01 Å to avoid some artefacts which are found for a circle of radius 0.02 Å.

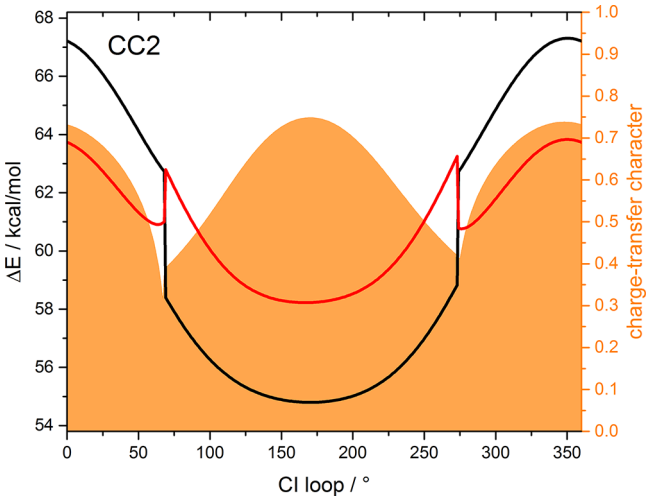

Figure S8 Energy profiles (in kcal/mol relative to *trans*-PSB3) of the reference state (black) and the response state (red) for the CC2 method along the circular path around the S_1/S_0 surface crossing of PSB3. For this circle, we used a radius of 0.03 Å, since this resulted in a continuous loop without any gaps due to unconverged points. The charge-transfer character of the reference state is shown in orange.

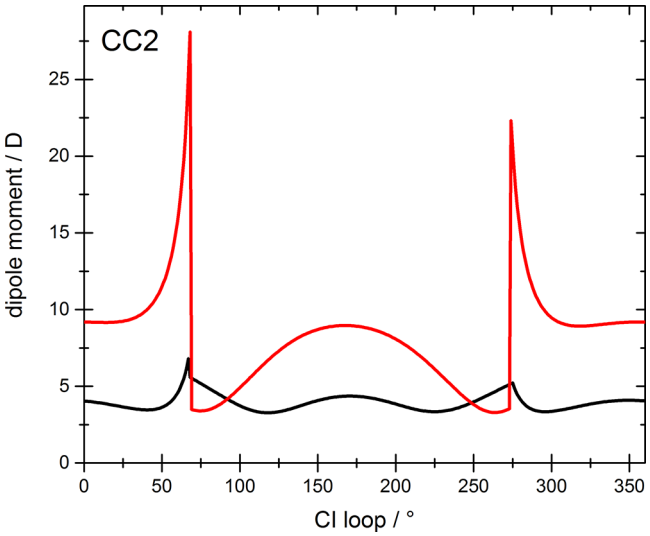

Figure S9 Dipole moments (in D) of the reference state (black) and of the response state (red) along the circular path around the surface crossing for the CC2 method.

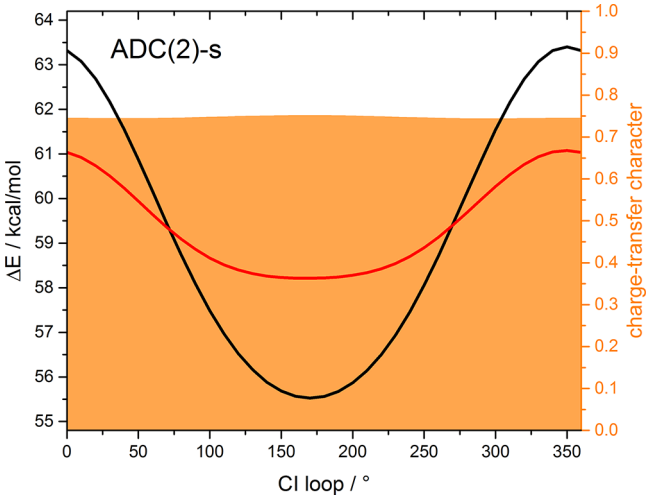

Figure S10 Energy profiles (in kcal/mol relative to *trans*-PSB3) of the reference state (black) and the response state (red) for the ADC(2)-s method along the circular path around the S_1/S_0 surface crossing of PSB3. The charge-transfer character of the reference state is shown in orange.

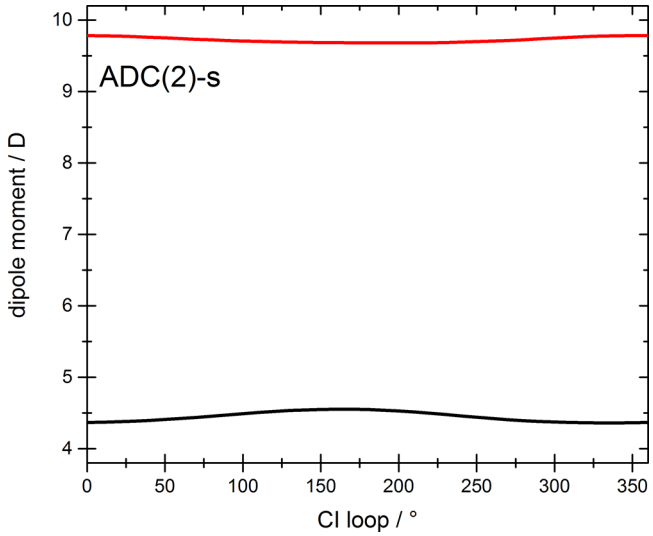

Figure S11 Dipole moments (in D) of the reference state (black) and the response state (red) along the circular path around the surface crossing for the ADC(2)-s method.

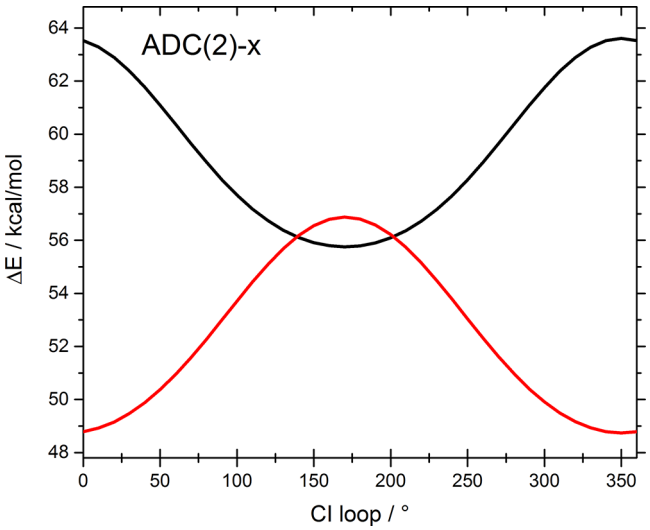

Figure S12 Energy profiles (in kcal/mol relative to *trans*-PSB3) of the reference state (black) and the response state (red) for the ADC(2)-x method along the circular path around the S_1/S_0 surface crossing of PSB3.

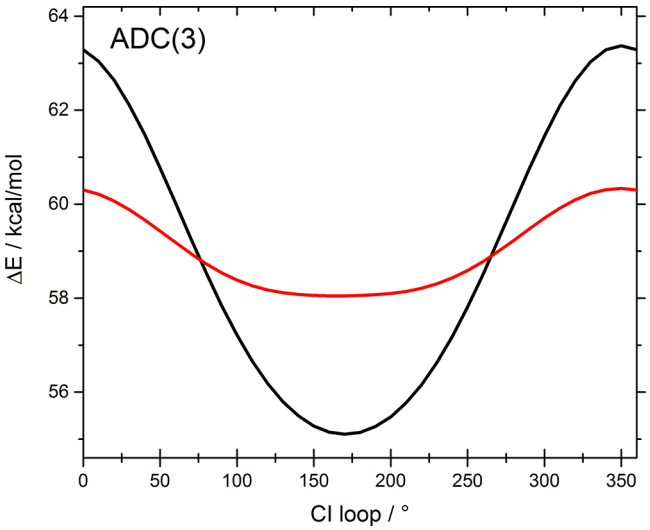

Figure S13 Energy profiles (in kcal/mol relative to *trans*-PSB3) of the reference state (black) and the response state (red) for the ADC(3) method along the circular path around the S_1/S_0 surface crossing of PSB3.

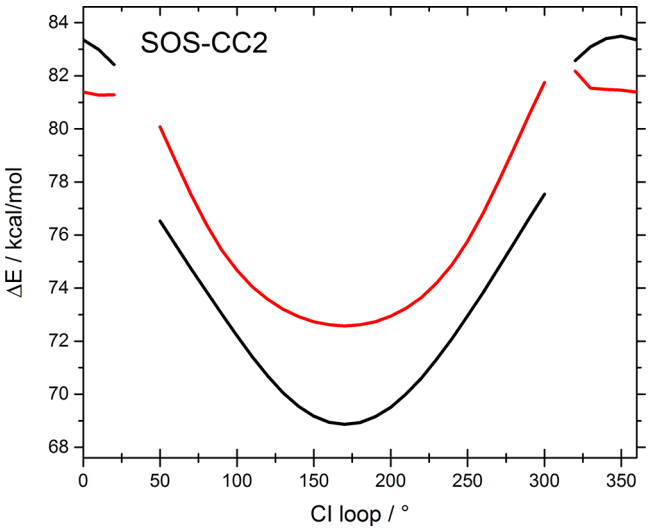

Figure S14 Energy profiles (in kcal/mol relative to *trans*-PSB3) of the reference state (black) and the response state (red) for the SOS-CC2 method along the circular path around the S_1/S_0 surface crossing of PSB3. The curves are discontinuous since a few points along the loop did not converge.

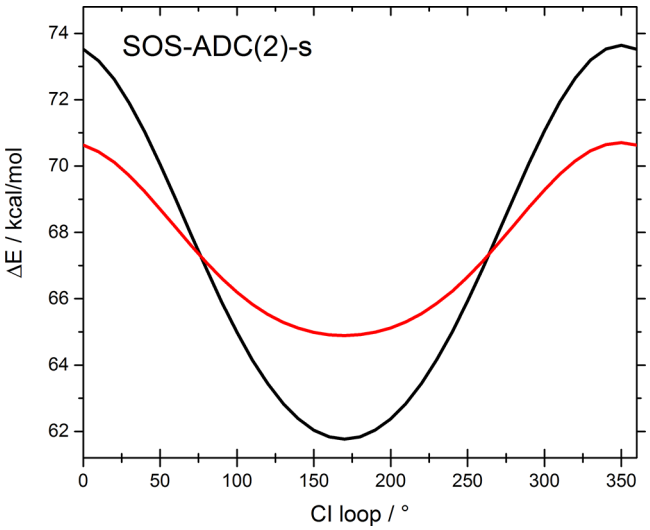

Figure S15 Energy profiles (in kcal/mol relative to *trans*-PSB3) of the reference state (black) and the response state (red) for the SOS-ADC(2)-s method along the circular path around the S_1/S_0 surface crossing of PSB3.

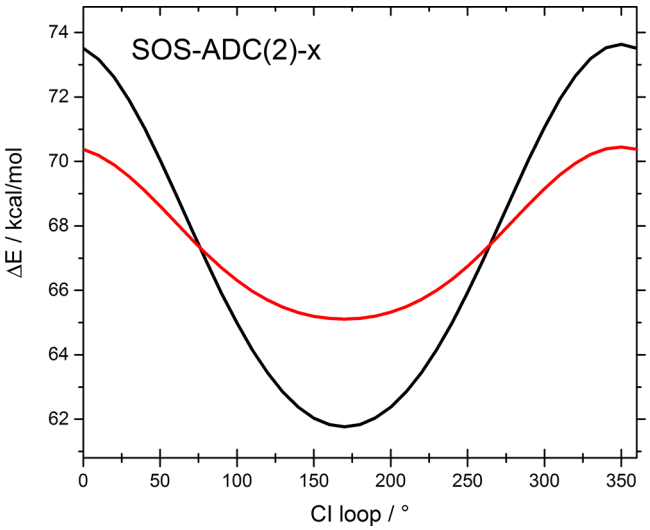

Figure S16 Energy profiles (in kcal/mol relative to *trans*-PSB3) of the reference state (black) and the response state (red) for the SOS-ADC(2)-x method along the circular path around the S_1/S_0 surface crossing of PSB3.

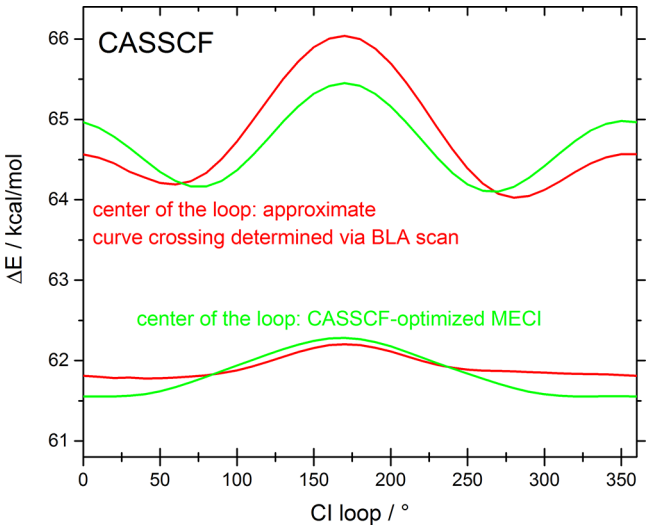

Figure S17 S_0 and S_1 energy profiles (in kcal/mol relative to *trans*-PSB3) for the CASSCF method along the circular path around the S_1/S_0 surface crossing of PSB3. The graph compares the effect of constructing the loop around the CASSCF-optimized minimum-energy conical intersection (which is shown in Figure S1 above; energy profiles shown in green) against constructing the loop around the approximate conical intersection determined via the BLA scan (which is shown in Figure 4 of the article; energy profiles shown in red).

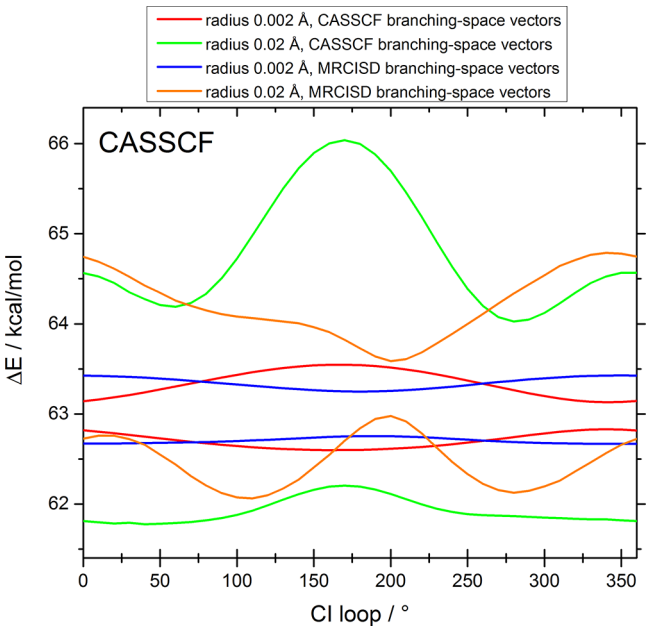

Figure S18 S_0 and S_1 energy profiles (in kcal/mol relative to *trans*-PSB3) for the CASSCF method along the circular path around the S_1/S_0 surface crossing of PSB3. The graph compares the effect of using a radius of 0.002 Å against a radius of 0.02 Å as well as using the orthonormalized CASSCF branching-space vectors against orthonormalized MRCISD branching-space vectors.

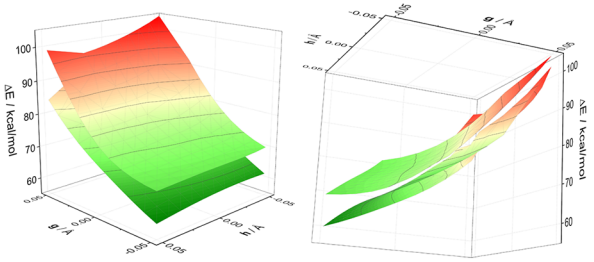

SOS-CC2

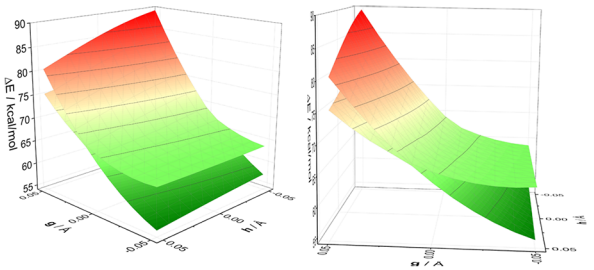

SOS-ADC(2)-s

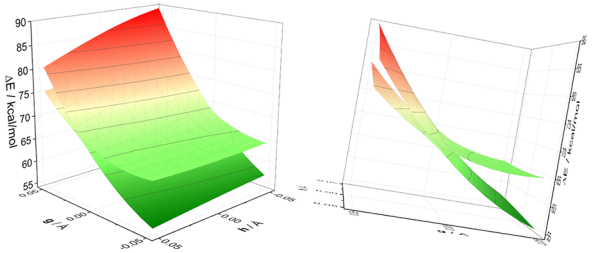

SOS-ADC(2)-x

Figure S19 Energy profiles (in kcal/mol) of the S_0 and S_1 adiabatic potential-energy surfaces in the two-dimensional branching space of the conical intersection of PSB3 (note that the energy scales are different for each plot) for the SOS variants of CC2, ADC(2)-s, and ADC(2)-x. The **g** vector corresponds roughly to the BLA coordinate, while the **h** vector corresponds roughly to the isomerization coordinate (cf. Figure S1). The grids were constructed by displacing the geometry of the approximate surface crossing determined via the BLA scan (shown in Figure 4 in the article) up to 0.05 Å in each direction along the orthonormalized **g** and **h** vectors (which were determined at the CASSCF level). For each method, the plot is shown from two different perspectives. At a few points along the constructed grids, the SOS-CC2 calculations did not converge, therefore a few points are missing for this method.

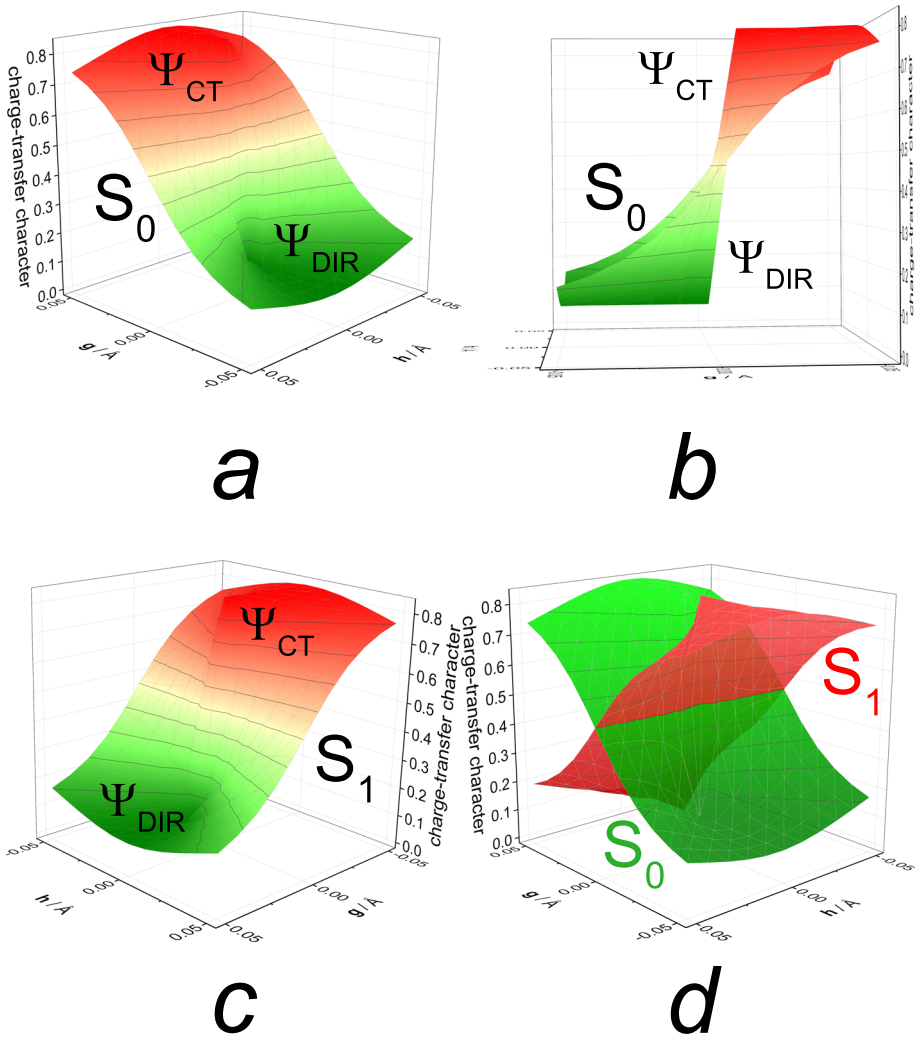

Figure S20 Charge-transfer character of the wavefunction computed at the MRCISD level along the two-dimensional branching space. The **g** vector corresponds roughly to the BLA coordinate, while the **h** vector corresponds roughly to the isomerization coordinate (cf. Figure S1). Two-dimensional plots are given for the ground-state adiabatic surface (S_0) from two perspectives (a) and (b), and for the excited-state adiabatic surface (S_1) from one perspective (c). It is shown that the wavefunction of the S_0 adiabatic state exhibits charge-transfer character where the wavefunction of the S_1 adiabatic state exhibits diradical character, and vice versa: the wavefunction of the S_0 adiabatic state exhibits diradical character where the wavefunction of the S_1 adiabatic state exhibits charge-transfer character. The reader should note the different perspectives of the plots shown in pictures (a) and (c). Picture (d) shows the charge-transfer character for both S_0 and S_1 adiabatic states in one plot for clarification.

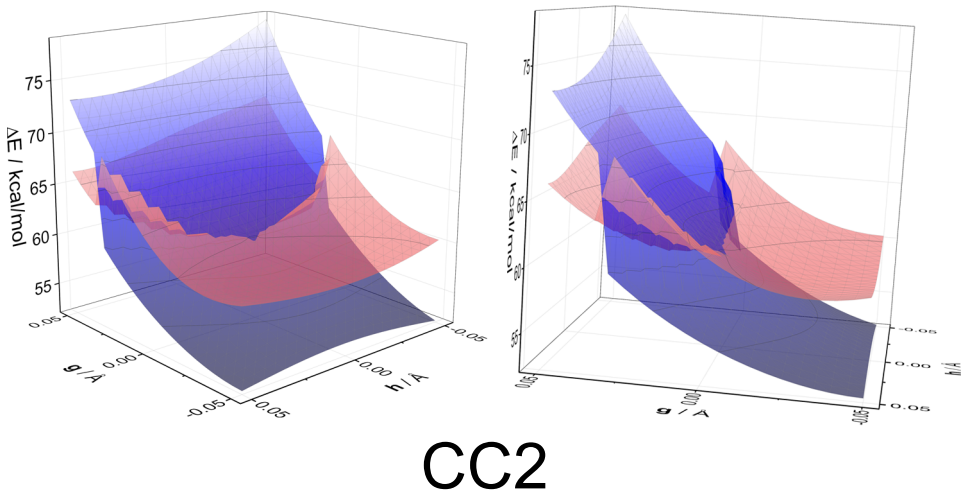

Figure S21 Potential-energy surfaces of the CC2 reference state (transparent blue surface) and the first CC2 response state (transparent red surface) in the two-dimensional branching space of the conical intersection of PSB3 shown from two different perspectives. These surfaces constitute the CC2 2D plot shown in Figure 10 in the article. The **g** vector corresponds roughly to the BLA coordinate, while the **h** vector corresponds roughly to the isomerization coordinate (cf. Figure S1).

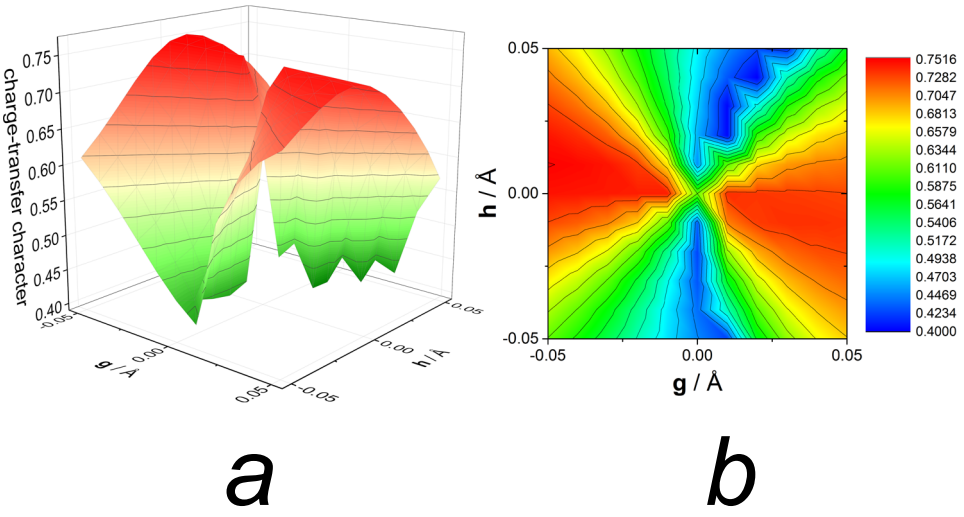

Figure S22 Charge-transfer character of the CC2 reference state along the two-dimensional branching space. The values of the charge-transfer character are shown as a two-dimensional plot (a) and as a contour plot (b). We remind the reader that the potential-energy surface of the CC2 reference state is the adiabatic S_0 state in some regions of the branching space, but the adiabatic S_1 state in other regions of the branching space (cf. Figure S22 below). The **g** vector corresponds roughly to the BLA coordinate, while the **h** vector corresponds roughly to the isomerization coordinate (cf. Figure S1).

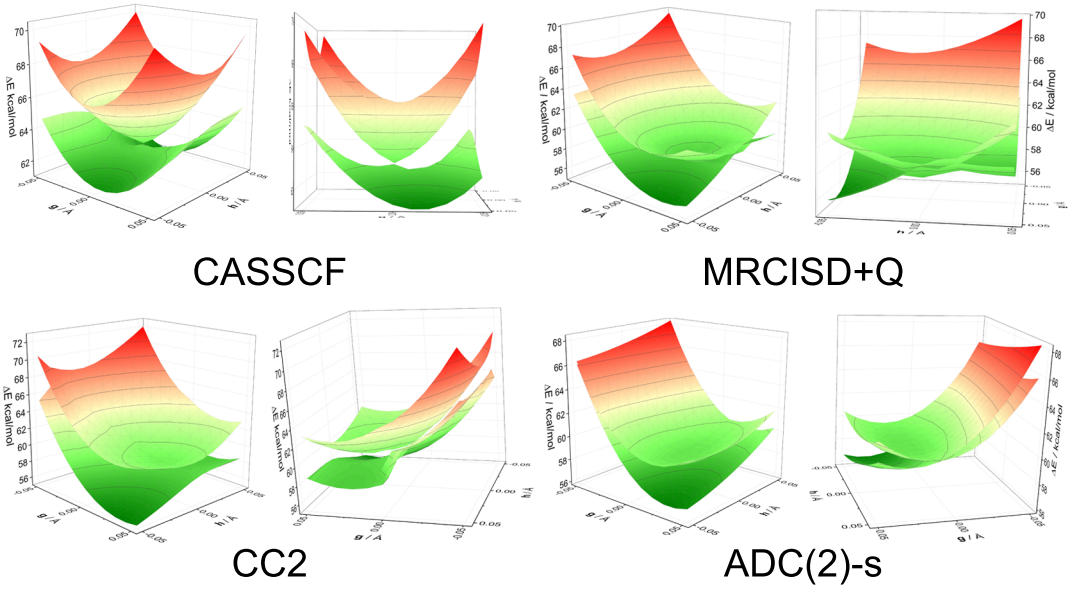

Figure S23 Selection of 2D potential-energy profiles along the branching space surrounding the conical intersection generated with the orthonormalized MR-CISD branching-space vectors (which are shown in Figure S1 above). The **g** vector corresponds roughly to the BLA coordinate, while the **h** vector corresponds roughly to the isomerization coordinate (cf. Figure S1). For CASSCF, the geometry of the CASSCF-optimized minimum-energy conical intersections was used as the center, while for MRCISD+Q, CC2, and ADC(2)-s, the geometries of the curve crossings determined via the BLA scan were used. For each method, the plot is shown from two different perspectives.

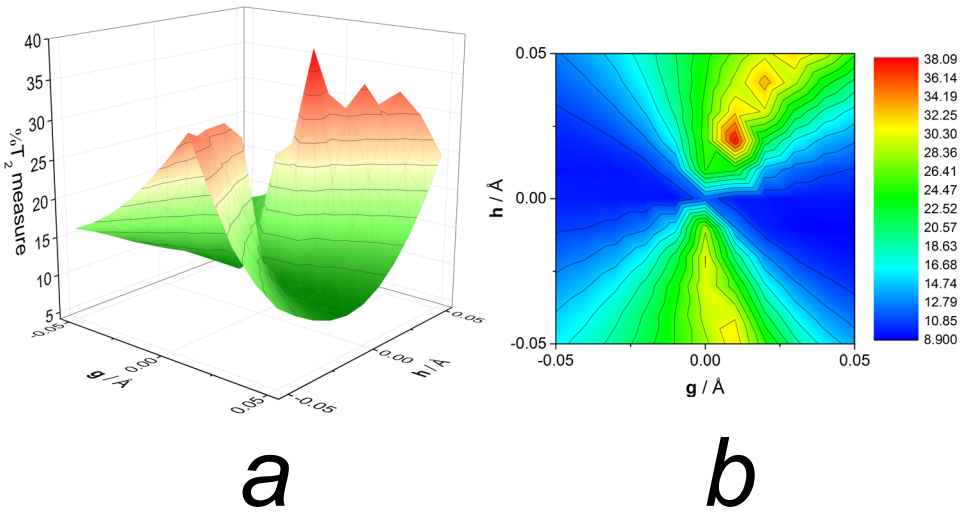

Figure S24 $\%T_2$ measure for the CC2 method along the two-dimensional branching space. The values of the $\%T_2$ measure are shown as a two-dimensional plot (a) and as a contour plot (b). The **g** vector corresponds roughly to the BLA coordinate, while the **h** vector corresponds roughly to the isomerization coordinate (cf. Figure S1).

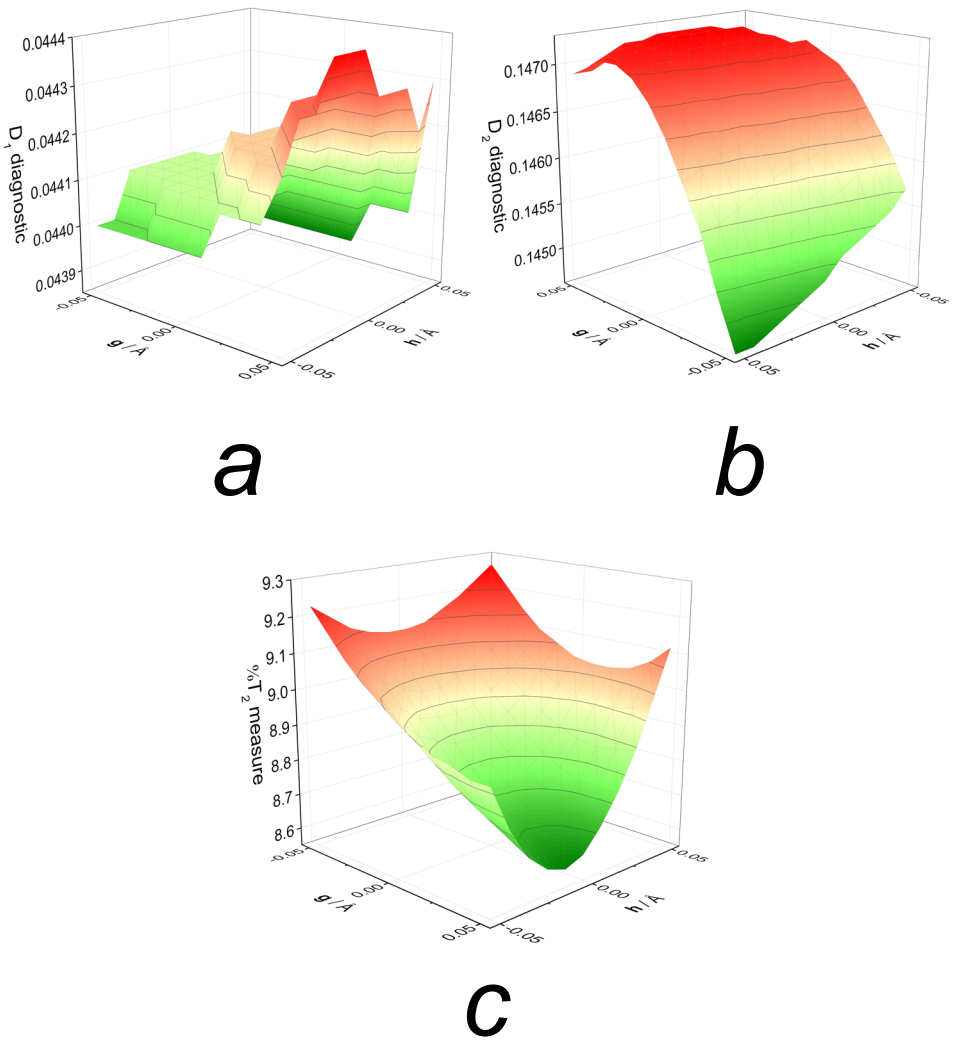

Figure S25 D_1 and D_2 diagnostics and $\%T_2$ measure for the ADC(2)-s method along the two-dimensional branching space. Two-dimensional plots are given for the D_1 diagnostic (a), the D_2 diagnostic (b), and the $\%T_2$ measure (c). Since the D_1 and D_2 diagnostics evaluate the ground-state reference wavefunction, these two diagnostics are evaluated for the MP2 method in the case of ADC(2)-s. The $\%T_2$ measure, on the other hand, is a diagnostic for an excited-state description of a linear-response method and therefore evaluates the properties of the ADC(2)-s method. The reader should note the narrow range of values for the diagnostics in comparison to the wide range shown for the CC2 method in Figure 12 in the article and in Figure S24 above. The **g** vector corresponds roughly to the BLA coordinate, while the **h** vector corresponds roughly to the isomerization coordinate (cf. Figure S1).

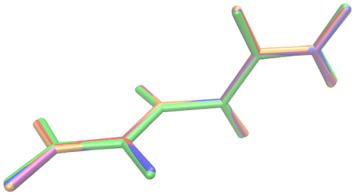

Figure S26 Superposition of the five geometries of the optimized or approximate minimum-energy conical intersections shown in Figure 14 of the article. Green: Page and Olivucci (2003), MS-CASPT2//CASSCF(6,6)/6-31G*; blue: Keal, Wanko, and Thiel (2009), MS-MR-CASPT2//CASSCF(6,6)/6-31G*; red: Nikiforov, Thiel, Filatov et al. (2014), MRCISD//CASSCF(4,4)/6-31+G**; orange: this work, CC2/6-31G*; purple: this work, ADC(2)/MP2/6-31G*.

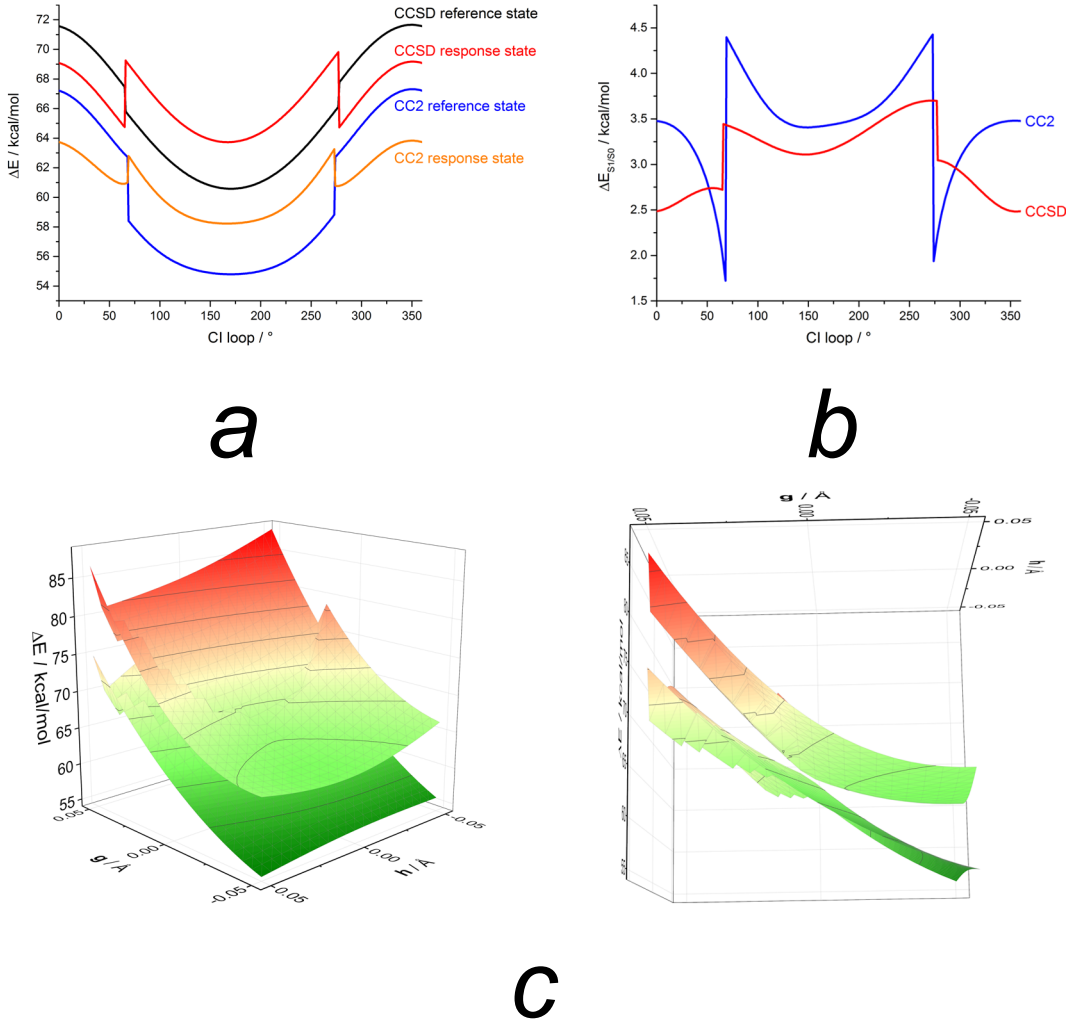

Figure S27 Comparison of the linear-response CCSD and CC2 methods along the circular path around the S_1/S_0 surface crossing of PSB3: (a) energy profiles (in kcal/mol relative to *trans*-PSB3) of the reference state (black for CCSD, blue for CC2) and the response state (red for CCSD, orange for CC2); (b) S_0-S_1 energy difference for the CCSD (red) and the CC2 (blue) method. Part (c) shows the energy profiles (in kcal/mol) of the S_0 and S_1 adiabatic potential-energy surfaces for the CCSD method in the two-dimensional branching space of the conical intersection of PSB3 from two perspectives. The **g** vector corresponds roughly to the BLA coordinate, while the **h** vector corresponds roughly to the isomerization coordinate (cf. Figure S1).

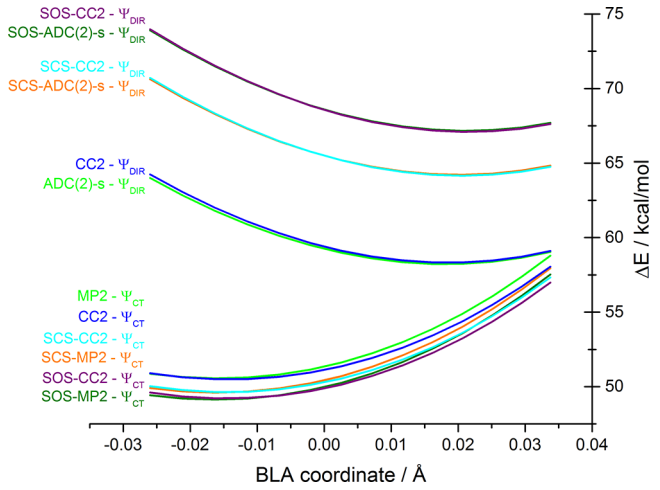

Figure S28 Energy profiles (in kcal/mol relative to *trans*-PSB3) of SCS and SOS variants of the CC2 and the ADC(2)-s methods along the BLA coordinate of PSB3. The curves are labelled at the left to distinguish diabatic potential-energy curves of mainly charge-transfer character (Ψ_{CT}) and covalent-diradical character (Ψ_{DIR}). The S_0 and S_1 energies are given for the CC2 method (blue), the SCS-CC2 method (cyan), the SOS-CC2 method (purple), the ADC(2)-s method (green), the SCS-ADC(2)-s method (orange), and the SOS-ADC(2)-s method (olive).

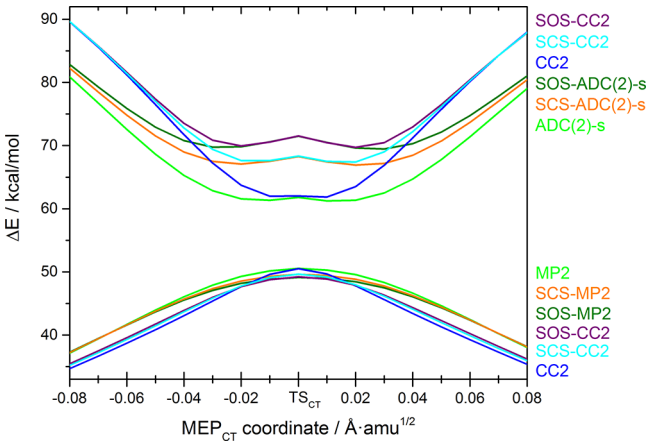

Figure S29 S_0 and S_1 energy profiles (in kcal/mol relative to *trans*-PSB3) along the MEP_{CT} pathway, which connects TS_{CT} (in the middle of the plot) with *cis*- and *trans*-PSB3. The energies are given for the CC2 method (blue), the SCS-CC2 method (cyan), the SOS-CC2 method (purple), the ADC(2)-s method (green), the SCS-ADC(2)-s method (orange), and the SOS-ADC(2)-s method (olive).

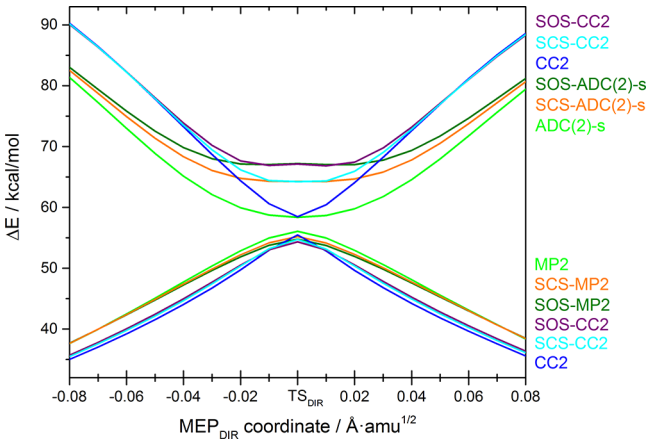

Figure S30 S_0 and S_1 energy profiles (in kcal/mol relative to *trans*-PSB3) along the MEP_{DIR} pathway, which connects TS_{DIR} (in the middle of the plot) with *cis*- and *trans*-PSB3. The energies are given for the CC2 method (blue), the SCS-CC2 method (cyan), the SOS-CC2 method (purple), the ADC(2)-s method (green), the SCS-ADC(2)-s method (orange), and the SOS-ADC(2)-s method (olive).

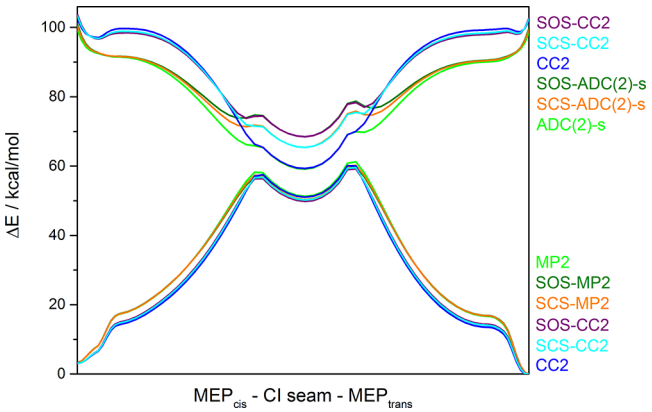

Figure S31 Energy profiles (in kcal/mol relative to *trans*-PSB3) along the composite CASPT2 S_1 pathway, which is composed of the MEP$_{cis}$, the CI-seam, and the MEP$_{trans}$ pathways. The S_0 and S_1 energies are given for the CC2 method (blue), the SCS-CC2 method (cyan), the SOS-CC2 method (purple), the ADC(2)-s method (green), the SCS-ADC(2)-s method (orange), and the SOS-ADC(2)-s method (olive).

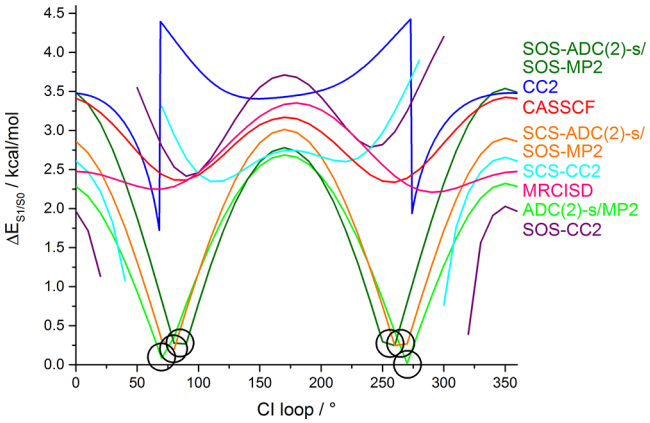

Figure S32 S_1–S_0 energy difference along a loop centered around the surface crossing of PSB3. Energy differences are given for the CC2 method (blue), the SCS-CC2 method (cyan), the SOS-CC2 method (purple), the ADC(2)-s method (green), the SCS-ADC(2)-s method (orange), the SOS-ADC(2)-s method (olive), and the reference methods CASSCF (red) and MRCISD+Q (black). A crossing of the two states along the loop results in a vanishing energy difference and is highlighted by black circles.

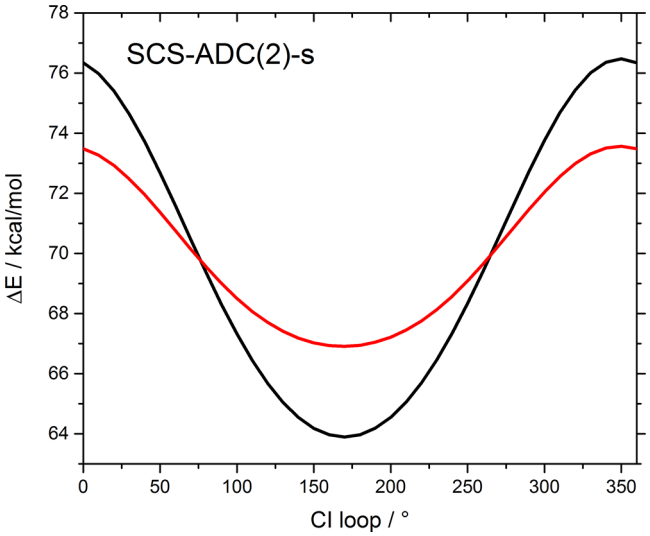

Figure S33 Energy profiles (in kcal/mol relative to *trans*-PSB3) of the reference state (black) and the response state (red) for the SCS-ADC(2)-s method along the circular path around the S_1/S_0 surface crossing of PSB3.

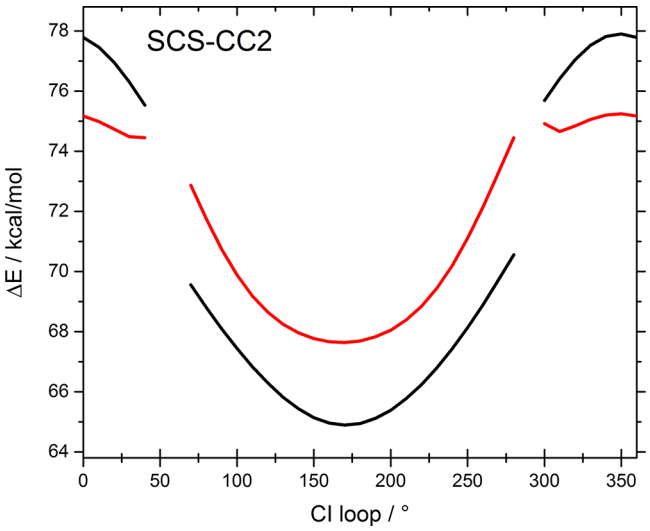

Figure S34 Energy profiles (in kcal/mol relative to *trans*-PSB3) of the reference state (black) and the response state (red) for the SCS-CC2 method along the circular path around the S_1/S_0 surface crossing of PSB3. The curves are discontinuous since a few points along the loop did not converge.

Table S2 Cartesian coordinates of the SA2-CASSCF/6-31G* optimized minimum-energy conical intersection of PSB3 (energy: $-248.154529\ E_h$).

```
14

C   -2.849345  -0.860488   0.801696
C   -1.474218  -0.904216   0.849965
C   -0.699999  -0.062027   0.046622
C    0.758118  -0.070105   0.028753
C    1.512781   0.750770   0.834238
N    2.837650   0.793113   0.845304
H    1.237733  -0.734019  -0.673351
H   -1.219155   0.606512  -0.623496
H    1.032415   1.420752   1.523496
H   -0.981849  -1.591094   1.513974
H    3.328120   1.410074   1.455539
H    3.391765   0.220217   0.244170
H   -3.448938  -1.500680   1.419810
H   -3.365571  -0.185269   0.144608
```

Table S3 Cartesian coordinates of the MRCISD//SA2-CASSCF(6,6)/6-31G* optimized minimum-energy conical intersection of PSB3 (energy: $-248.151506\ E_h$).

```
14

C   -0.01204623  -0.02476853  -0.01049300
C    1.37386577   0.02603082   0.00212517
C    2.17877635  -1.10392947   0.12839782
C    3.63595224  -1.04163132   0.17550314
C    4.42764314  -1.16301731  -0.98491563
N    5.73623135  -1.12094111  -0.96205270
H    4.14758307  -0.91695374   1.12587100
H    1.72313958  -2.07956914   0.25694087
H    3.96426218  -1.29411619  -1.95251134
H    1.85219285   0.99271791  -0.09149682
H    6.28286457  -1.20768095  -1.80881860
H    6.25187621  -1.00157557  -0.09843136
H   -0.59948223   0.87208628  -0.11345123
H   -0.54030211  -0.96091395   0.08494226
```

Table S4 Cartesian coordinates of the CC2/6-31G* optimized minimum-energy conical intersection of PSB3 (energy: $-248.892573\ E_h$).

```
14

C   -2.8694664425  -0.8923771527   0.8236068206
C   -1.4854483069  -0.8691516150   0.8184106348
C   -0.7228690962  -0.0146979326   0.0249847949
C    0.7411188025  -0.0554644534   0.0156586985
C    1.5131684089   0.8018036268   0.8730039411
N    2.8223708850   0.7747869349   0.8594746776
H    1.3205216588  -0.7210310651  -0.6393260011
H   -1.1768536611   0.6534592388  -0.7089451999
H    1.0156637392   1.4908714069   1.5537405878
H   -0.9670439968  -1.5571673855   1.4913226188
H    3.3756290064   1.3836734575   1.4693892730
H    3.3447239894   0.1451062741   0.2406860242
H   -3.4219496415  -1.5672798055   1.4668506252
H   -3.4340953549  -0.2306715252   0.1708324997
```

Table S5 Cartesian coordinates of the [ADC(2)-s/MP2]/6-31G* optimized minimum-energy conical intersection of PSB3 (energy: $-248.879799\ E_h$).

```
14

C   -2.8600576360  -0.8888861069   0.8202563662
C   -1.4830833605  -0.8706261740   0.8230225193
C   -0.7167372675  -0.0183456926   0.0236243679
C    0.7396287033  -0.0542593556   0.0197890066
C    1.5114441030   0.7981328527   0.8705578682
N    2.8155603983   0.7723785528   0.8583501472
H    1.3111457263  -0.7179059418  -0.6347069318
H   -1.1830039011   0.6545180230  -0.7021745196
H    1.0137873993   1.4857481917   1.5474583524
H   -0.9640178178  -1.5591471291   1.4937218595
H    3.3695263239   1.3827416017   1.4664284061
H    3.3447895566   0.1474137068   0.2432970526
H   -3.4167471640  -1.5631850990   1.4619822989
H   -3.4267650695  -0.2266873836   0.1680831766
```